A POLYAXIAL STRESS-STRAIN LAW FOR ATJS GRAPHITE

AEROSPACE CORPORATION

PREPARED FOR
SPACE AND MISSILE SYSTEMS ORGANIZATION

23 JANUARY 1975

UNCLASSIFIED

SECURITY CLASSIFICATION OF THIS PAGE (When Data Entered)

REPORT DOCUMENTATION PAGE		READ INSTRUCTIONS BEFORE COMPLETING FORM
1. REPORT NUMBER SAMSO-TR-75-39	2. GOVT ACCESSION NO.	3. RECIPIENT'S CATALOG NUMBER AD/A005633
4. TITLE (and Subtitle) A POLYAXIAL STRESS-STRAIN LAW FOR ATJS GRAPHITE		5. TYPE OF REPORT & PERIOD COVERED Interim 6. PERFORMING ORG. REPORT NUMBER TR-0075(5450-76)-2
7. AUTHOR(s) Samuel B. Batdorf		8. CONTRACT OR GRANT NUMBER(s) F04701-74-C-0075
9. PERFORMING ORGANIZATION NAME AND ADDRESS The Aerospace Corporation El Segundo, Calif. 90245		10. PROGRAM ELEMENT, PROJECT, TASK AREA & WORK UNIT NUMBERS
11. CONTROLLING OFFICE NAME AND ADDRESS Space and Missile Systems Organization Air Force Systems Command Los Angeles, Calif. 90045		12. REPORT DATE 28 January 1975 13. NUMBER OF PAGES 29
14. MONITORING AGENCY NAME & ADDRESS(if different from Controlling Office)		15. SECURITY CLASS. (of this report) Unclassified 15a. DECLASSIFICATION/DOWNGRADING SCHEDULE

16. DISTRIBUTION STATEMENT (of this Report)

Approved for public release; distribution unlimited

17. DISTRIBUTION STATEMENT (of the abstract entered in Block 20, if different from Report)

18. SUPPLEMENTARY NOTES

PRICES SUBJECT TO CHANGE

19. KEY WORDS (Continue on reverse side if necessary and identify by block number)

Graphite Stress-Strain Laws
Polyaxial Stress-Strain Laws
Stress-Strain Laws

20. ABSTRACT (Continue on reverse side if necessary and identify by block number)

Theoretical considerations are applied to Jortner's experimental data in order to develop a simple analytical stress-strain relation for ATJS under arbitrary loading conditions. Since correlation with the entire range of proportional loading data is good, it is reasonable to expect that the theoretical predictions of strains for stresses that are inaccessible in the laboratory will also be good. It is anticipated that, with minor changes in the values of the theoretical parameters, the stress-strain law will also apply to other transversely isotropic graphites.

DD FORM 1473 (FACSIMILE)

UNCLASSIFIED

SECURITY CLASSIFICATION OF THIS PAGE (When Data Entered)

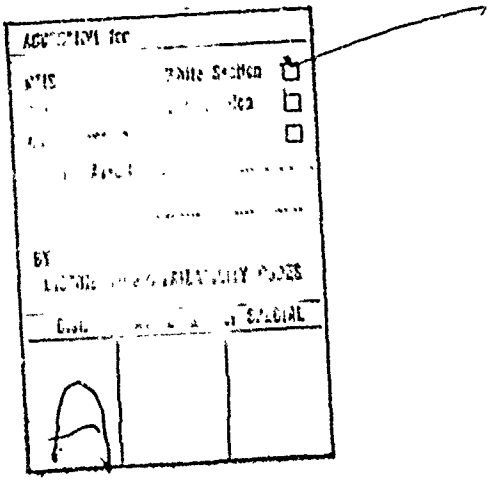

Approved

G. W. King, Vice President
and General Manager
Laboratory Operations

R. G. Allen, Group Director
Ballistic Reentry Vehicles
Group Directorate
Reentry Systems Division

Publication of this report does not constitute Air Force Approval of the report's findings or conclusions. It is published only for the exchange and stimulation of ideas.

James E. Green, Capt., USAF
Aero & Materials Division
Directorate of Systems Engineering
Deputy for Reentry Systems

PREFACE

This work was performed for the Ballistic Vehicles Group Directorate, Reentry Systems Division, Development Operations.

CONTENTS

TABLE

FIGURES

I. INTRODUCTION

The stress analysis of an arbitrarily loaded solid body can only be performed if the stress-strain relations are known for an arbitrary polyaxial stress state. In the case of isotropic, linearly elastic materials, the stress-strain law is completely defined by two constants, commonly Young's modulus and Poisson's ratio. In ATJS and related graphites, the situation is far more complicated because they are neither linear nor isotropic. In addition, there are some differences between compressive and tensile behavior. As it is not feasible to determine experimentally the stress-strain relation for all possible stress states, it is necessary to combine a limited number of test data with theoretical considerations in order to develop a general stress-strain law.

One of the most extensive sets of test data for ATJS graphite under combined stresses was obtained by J. Jortner.[1-5] These tests were performed at normal and elevated temperature on both cylindrical shells and solid-bar specimens. Proportional loading tests were performed that included uniaxial stresses, biaxial stresses, and a limited number of triaxial stress states. Also included were tests involving nonproportional loading.

Among the major conclusions from these tests were the following:

1. The classical theory of plasticity does not apply to ATJS because classical plasticity assumes that inelastic strain is isovolumetric, a behavior not encountered in this type of graphite. In addition, the usual rule in incremental plasticity theory that plastic strain is normal to surfaces of constant plastic potential is not obeyed.

2. The strain ratios remain approximately constant during proportional loading in compression. In the case of tension, the same is true except for uniaxial or nearly uniaxial stress states.
3. ATJS exhibits "strain softening," i.e., the strains tend to be larger under biaxial tension than under uniaxial tension.
4. The tensile stress-strain curve is always concave downward, i.e., the tangent modulus continually decreases with increasing stress. The compressive stress-strain curve is concave downward at stresses equal in absolute magnitude or less than the tensile fracture stress. In this stress range, the behavior is quite similar to the behavior in tension except for Poisson effects. At much higher stresses, the curve flattens out, and there may even be an inflection point.

Because classical plasticity theory was found to be inapplicable, the main theoretical guidance in developing a stress-strain law comes from a consideration of two limiting cases. For sufficiently small stresses, the theory should reduce to the appropriate orthotropic elastic theory; and, at any stress, the equations should be invariant to a rotation of axes when the anisotropy is reduced to zero. A heuristic account of the development of such a stress-strain law is contained in the following section. Only room-temperature properties are considered, and attention is limited to stress states in which no compressive stress is much in excess of the absolute value of the tensile fracture stress.

II. DEVELOPMENT OF STRESS-STRAIN LAW

In the case of a transversely isotropic elastic solid, such as ATJS at very low stresses, the stress-strain law is essentially linear and can be written in cylindrical coordinates as:[6]

$$\epsilon_z = \frac{\sigma_z}{E'} - \frac{\nu'}{E'}\,\sigma_\theta - \frac{\nu'}{E'}\,\sigma_r \quad , \tag{1a}$$

$$\epsilon_\theta = -\frac{\nu'}{E'}\,\sigma_z + \frac{\sigma_\theta}{E} - \frac{\nu}{E}\,\sigma_r \quad , \tag{1b}$$

$$\epsilon_r = -\frac{\nu'}{E'}\,\sigma_z - \frac{\nu}{E}\,\sigma_\theta + \frac{\sigma_r}{E} \quad , \tag{1c}$$

$$\gamma_{\theta z} = \frac{1}{G'}\,\tau_{\theta z} \quad , \tag{1d}$$

$$\gamma_{rz} = \frac{1}{G'}\,\tau_{rz} \quad , \tag{1e}$$

and

$$\gamma_{r\theta} = \frac{1}{G}\,\tau_{r\theta} = \frac{2(1+\nu)}{E}\,\tau_{r\theta} \quad . \tag{1f}$$

In the above equations, z is chosen in the cross-grain direction, while r and θ define the plane of symmetry, in which with-grain properties apply. The matrix relating stress and strain is symmetric, a property which follows from the existence of an elastic potential. The values of the constants for ATJS have been listed[3] as approximately:

$$E = E_r = E_\theta = E_{WG} = 1.8 \times 10^6 \text{ psi} \quad , \tag{2a}$$

$$E' = E_z = E_{CG} = 1.2 \times 10^6 \text{ psi} \quad , \tag{2b}$$

$$\nu = \nu' = 0.10 \quad , \tag{2c}$$

$$G = G_{r\theta} = 8 \times 10^5 \text{ psi} \quad , \tag{2d}$$

and

$$G' = G_{zr} = G_{z\theta} = 6.5 \times 10^5 \text{ psi} \quad . \tag{2e}$$

Thus,

$$\frac{\nu'}{E'} = 8.3 \times 10^{-8} \text{ (psi)}^{-1} \tag{2f}$$

and

$$\frac{\nu}{E} = 5.6 \times 10^{-8} \text{ (psi)}^{-1} \quad . \tag{2g}$$

So that these results can be extended into the nonlinear range, uniaxial tension is first considered. Test results that give longitudinal and transverse strain as a function of stress are presented in Figs. 1 and 2 for with-grain and cross-grain loading, respectively.[5] It should be noted that the transverse strain is small and approximately proportional to the loading. Consequently, it is assumed that in tension the Poisson effect behaves elastically.

The longitudinal strain is nonlinearly related to the stress, but the elastic limit varies widely from specimen to specimen and is in many cases difficult to determine accurately. In cases in which the nonlinearity seems to start imperceptibly at very low stress, the data can be fitted quite well with the assumption that inelastic strain is proportional to the square of the

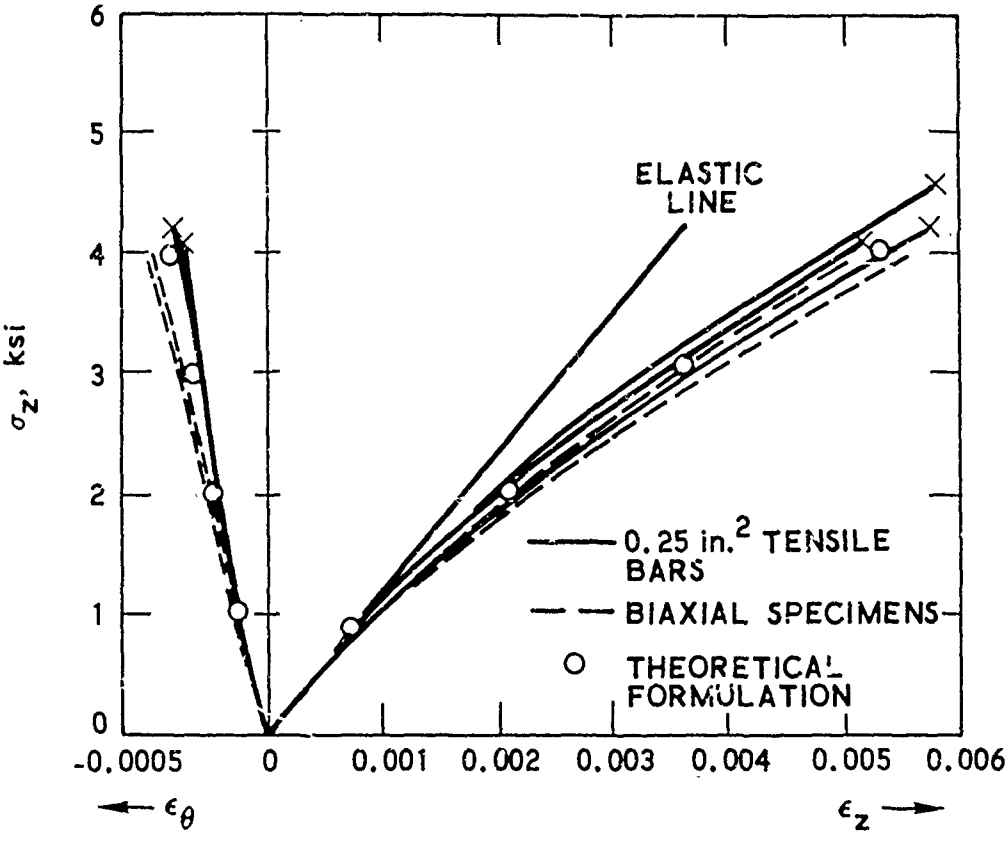

Fig. 1. With-Grain Tension S'rain Response of ATJS at 70°F (adapted from reference cited in footnote 5)

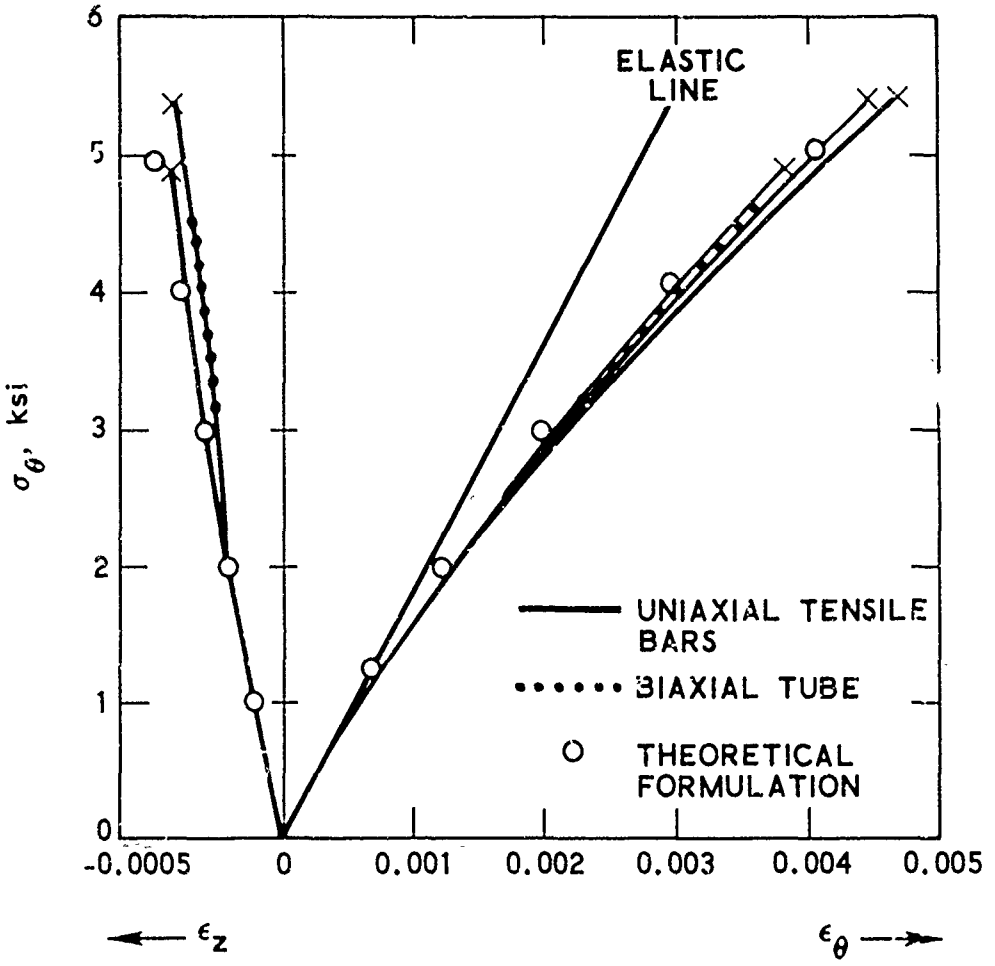

Fig. 2. Across-Grain Tension Strain Response of ATJS at 70°F (adapted from reference cited in footnote 5)

stress. A compatible assumption for cases in which an elastic limit stress exists is that the inelastic strain is given by

$$\epsilon_i = K \frac{\sigma}{E} \left(\frac{\sigma}{\sigma^0} - 1 \right) \quad , \tag{3}$$

where σ^0 is the elastic limit stress. When K is chosen to give the correct inelastic strain at fracture, Eq. (3) generally leads to good agreement over the entire stress-strain curve. It turns out that K = 0.15 leads to reasonable average values for the elastic limit as well as the observed inelastic strains at fracture, as can be seen in Figs. 1 and 2. In practice, then, the elastic limit is determined by requiring Eq. (3) to be satisfied at fracture and solving it for σ^0. The result is

$$\sigma^0 = \frac{\sigma_{\text{fracture}}}{1 + 6.7 \left(\epsilon_i / \epsilon_e \right)_{\text{fracture}}} \quad , \tag{4}$$

where ϵ_e and ϵ_i are the elastic and inelastic longitudinal strains, respectively. Although σ^0 found in this manner will not in general exactly coincide with the highly variable observed elastic limit, the error in total strain resulting from the discrepancy will be so small as to be negligible in most cases.

Next, the question is addressed: How should this approach to biaxial tension be generalized? A plausible expression that reduces to Eq (3) in the uniaxial limit is

$$\left(\epsilon_x \right)_i = F \frac{\sigma_x}{E_x} \quad , \tag{5}$$

where

$$F = 0.15\left\{\left[\left(\frac{\sigma_x}{\sigma_{x0}}\right)^n + \left(\frac{\sigma_y}{\sigma_{y0}}\right)^n\right]^{1/n} - 1\right\} \qquad (6)$$

when the bracketed expression is positive, and F = 0 when it is negative. The choice of n will determine the amount of "strain softening." Table I gives biaxial stress and strain data for ATJS at fracture. Figure 3 shows the fracture strains computed from the experimental stresses when n = 2. The agreement between calculated and measured strains is quite good, probably as good as can be expected when the variations in properties between specimens are considered. In addition to this empirical reason for choosing n = 2, there is a theoretical reason that follows.

Since the biaxial experiments just cited did not include shear, they do not provide a check on whether shear should be included in a general expression for F. However, one would expect that, as anisotropy is reduced to zero, F should be invariant with respect to a rotation of axes. An invariant expression that reduced to a sum of squares of the direct stresses in the principal axis system is

$$J_1^2 + 2J_2 = \Sigma\sigma_i^2 + \sum_{i\neq j} \tau_{ij}^2 \quad , \qquad (7)$$

where J_1 and J_2 are the first and second stress invariants, respectively. Thus, a plausible expression for F in the general case becomes

Table I. Jortner's Biaxial Failure Data[a]

σ_z/σ_θ	σ_z(ksi)	σ_θ (ksi)	ϵ_z	ϵ_θ
1:0	3.940	0	0.00548	-0.00038
1:1.26	3.358	4.246	0.00462	0.00348
0:1	0	4.786	-0.00033	0.0039
-1:1	-4.120	4.220	-0.0063	0.0043

[a]Each value listed is the average of three to five experiments.

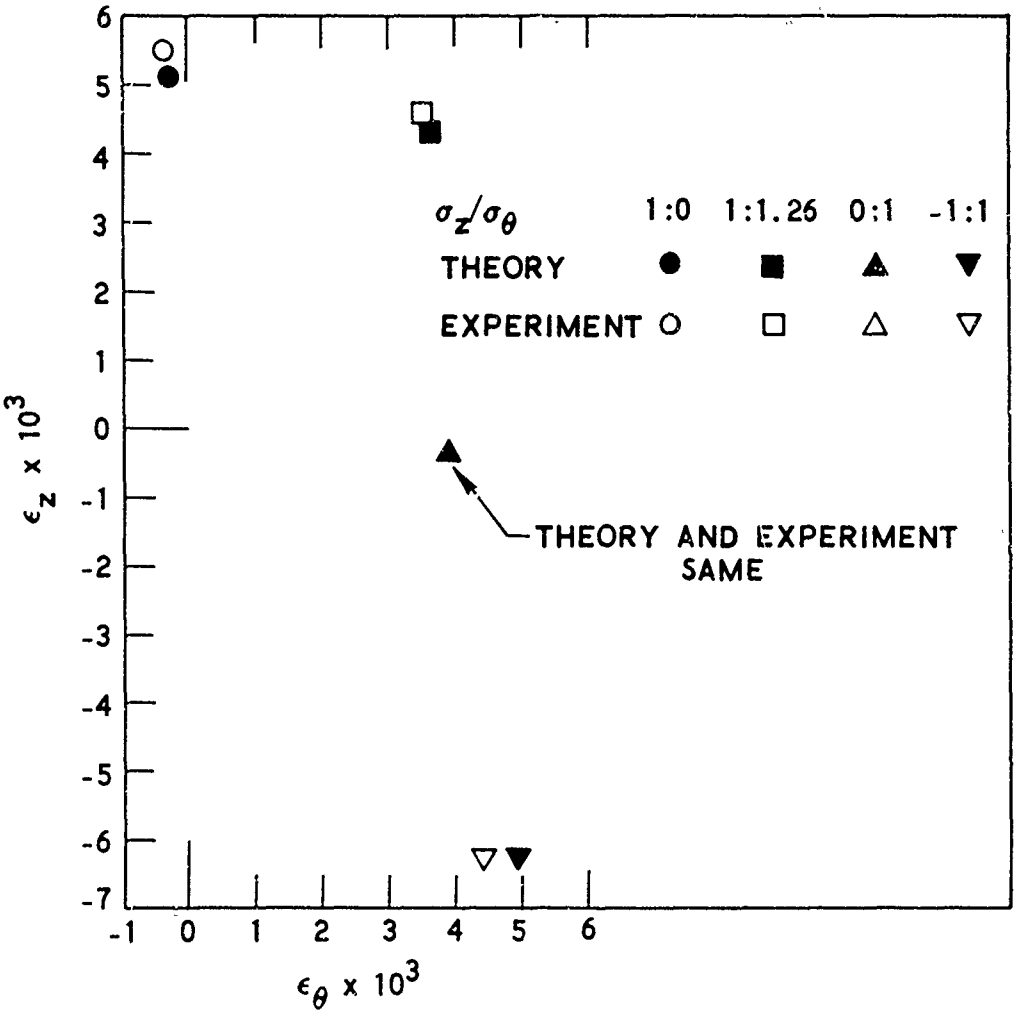

Fig. 3. Comparison of Measured and Computed Fracture Strains Under Biaxial Loading

$$F = 0.15 \left\{ \left[\left(\frac{\sigma_z}{\sigma_z^0} \right)^2 + \left(\frac{\sigma_\theta}{\sigma_\theta^0} \right)^2 + \left(\frac{\sigma_r}{\sigma_r^0} \right)^2 + 2 \left(\frac{\tau_{z\theta}^2}{\sigma_z^0 \sigma_\theta^0} + \frac{\tau_{zr}^2}{\sigma_z^0 \sigma_r^0} + \frac{\tau_{r\theta}^2}{\sigma_r^0 \sigma_\theta^0} \right) \right]^{1/2} - 1 \right\} \quad (8)$$

when the bracketed expression is positive, and F = 0 when it is negative.

With this definition of F, the general stress-strain law for tension becomes:

$$\epsilon_z = \frac{\sigma_z}{E'} (1 + F) - 8.3 \times 10^{-8} (\sigma_\theta + \sigma_r) \quad , \quad (9a)$$

$$\epsilon_\theta = -8.3 \times 10^{-8} \sigma_z + \frac{\sigma_\theta}{E} (1 + F) - 5.6 \times 10^{-8} \sigma_r \quad , \quad (9b)$$

$$\epsilon_r = -8.3 \times 10^{-8} \sigma_z - 5.6 \times 10^{-8} \sigma_\theta + \frac{\sigma_r}{E} (1 + F) \quad , \quad (9c)$$

$$\gamma_{0z} = (1 + F) \frac{\tau_{\theta z}}{G'} \quad , \quad (9d)$$

$$\gamma_{rz} = (1 + F) \frac{\tau_{rz}}{G'} \quad , \quad (9e)$$

and

$$\gamma_{r\theta} = (1 + F) \frac{\tau_{r\theta}}{G} \quad . \quad (9f)$$

Note that the values for E and G are given in Eq. (2). The constants needed to determine F were found, in fitting the tensile curves of Figs. 1 and 2, to be

$$\sigma_z^0 = 0.82 \text{ ksi} \tag{10a}$$

and

$$\sigma_r^0 = \sigma_\theta^0 = 1.22 \text{ ksi} \quad . \tag{10b}$$

It was found[3] that the compressive stress-strain curve was close to the tensile curve, but that the Poisson effect was quite different. In compression, the transverse strain was proportional to the longitudinal strain, rather than to the longitudinal stress. Accordingly, under combined compressive stresses, the stress-strain law is assumed to be:

$$\epsilon_z = (1 + F)\left[\frac{\sigma_z}{E} - 8.3 \times 10^{-8} (\sigma_\theta + \sigma_r)\right] \quad , \tag{11a}$$

$$\epsilon_\theta = (1 + F)\left(-8.3 \times 10^{-8} \sigma_z + \frac{\sigma_\theta}{E} - 5.6 \times 10^{-8} \sigma_r \right) \quad , \tag{11b}$$

$$\epsilon_r = (1 + F)\left(-8.3 \times 10^{-8} \sigma_z - 5.6 \times 10^{-8} \sigma_\theta + \frac{\sigma_r}{E} \right) \quad , \tag{11c}$$

$$\gamma_{\theta z} = (1 + F)\frac{\tau_{\theta z}}{G'} \quad , \tag{11d}$$

$$\gamma_{rz} = (1 + F)\frac{\tau_{rz}}{G'} \quad , \tag{11e}$$

and

$$\gamma_{r\theta} = (1 + F)\frac{\tau_{r\theta}}{G} \quad , \tag{11f}$$

The only difference between the equations for tension and those for compression lies in the off-diagonal terms that give the Poisson effect. In mixed states involving both compression and tension, the Poisson term associated with a compressive stress will be calculated as in Eq. (11), while the Poisson term associated with a tensile stress will be calculated as in Eq. (9).

III. COMPARISON WITH TRIAXIAL STRESS DATA

The stress-strain laws just formulated were based on uniaxial tests in compression and tension, and on general theoretical considerations. Their form implies superposition of Poisson effects. While such superposition is a requirement when the relations are linear, it cannot be assumed to be valid in the nonlinear case with which this paper is concerned. It therefore can only be used with confidence if experimentally confirmed. Such confirmation was shown in the preceding section in the case of biaxial fracture data in tension. Now the equations will be checked against triaxial proportional loading experiments in which the stresses in the plane of symmetry are equal compressions and the stress in the cross-grain direction can be either tensile or compressive in nature.

The test data from the triaxial tests are shown in Fig. 4, which is taken from the reference cited in footnote 5. Superposed on the experimental curves are calculated points based on the use of Eqs. (9) and (11). The good agreement between theory and experiment appears to validate both the above-noted necessity of two different treatments of the Poisson effect, depending on whether the associated stress is positive or negative, and the assumption of superposition of Poisson effects. It also appears to indicate that the nonlinear coupling between stress components, which is assumed in Eq. (8), is at least approximately correct. In making this comparison, it was noted that the specimens were bars and that bars were slightly stiffer in the cross-grain direction than the cylinders to which the uniaxial laws were tailored. To account for this, σ_z^0 was taken to be 1.04 ksi.

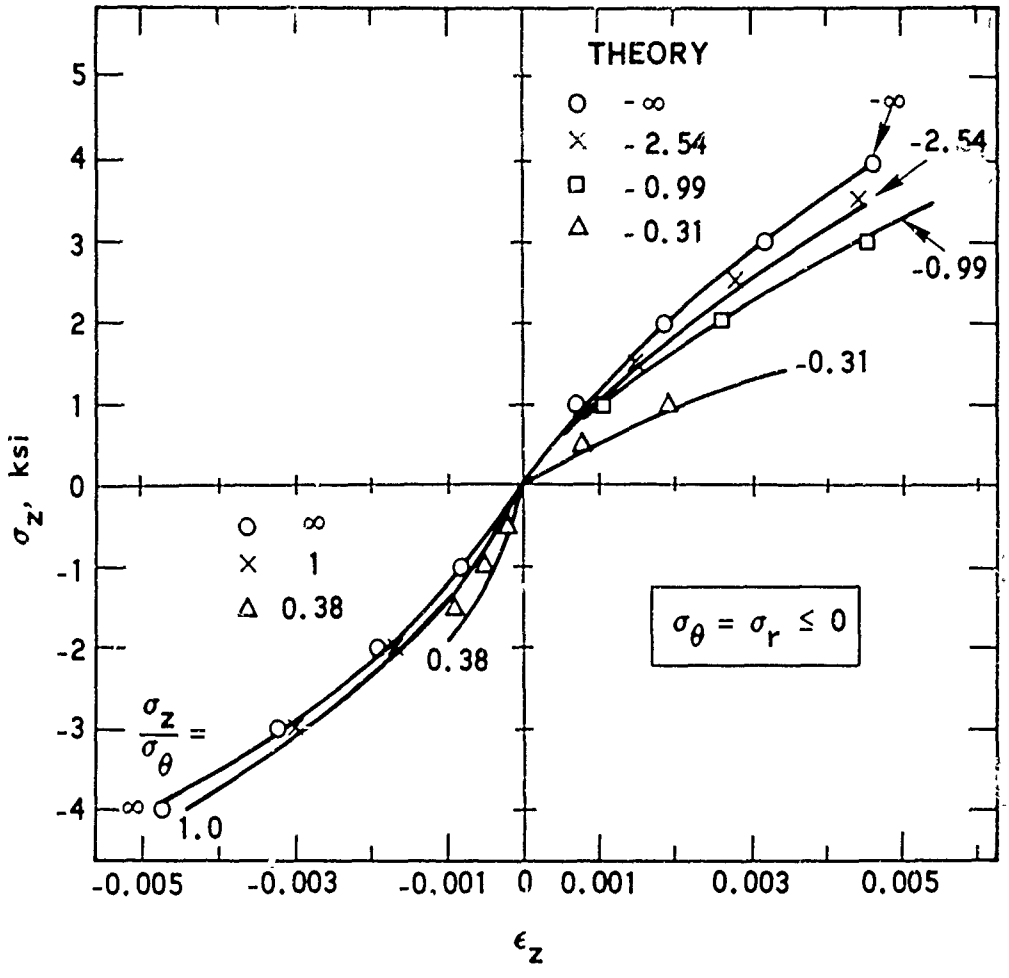

Fig. 4. Across-Grain Stress-Strain Responses, Triaxial Tests, Compared with Theory (adapted from reference cited in footnote 5)

IV. NONPROPORTIONAL LOADING

All the data discussed up to this point were obtained from proportional loading tests, and the equations developed to represent them are in finite rather than incremental form. Such a form is appropriate for proportional loading, but if the inelastic strains associated with a given stress state depend significantly on the loading path, the equations just developed cannot be used for nonproportional loading.

Nonproportional loading paths and the corresponding strains are shown in Figs. 5 and 6, respectively, taken from the reference cited in footnote 5. The fact that three different loading paths to the same final stress state led to three different strain states suggests some path dependence, but the evidence is really not clear. Incremental plasticity theory would predict that, when a specimen is first loaded in one direction and then a load is added at right angles, the strain in the first direction will be bigger than if the loads are applied in the reverse order. This qualitative prediction is fulfilled in the case of ϵ_z but not in the case of ϵ_θ. Straightforward application of the equations of the present paper to path bx of Fig. 5 leads to the data represented by the triangles shown in Fig. 6. It is evident from a comparison of theory and experiment for point b that specimen 87 was somewhat weaker in the cross-grain direction than assumed in the theory, which could account for the discrepancies in the remaining points. In any event, it is possible to show from very general considerations (omitted here for the sake of brevity) that

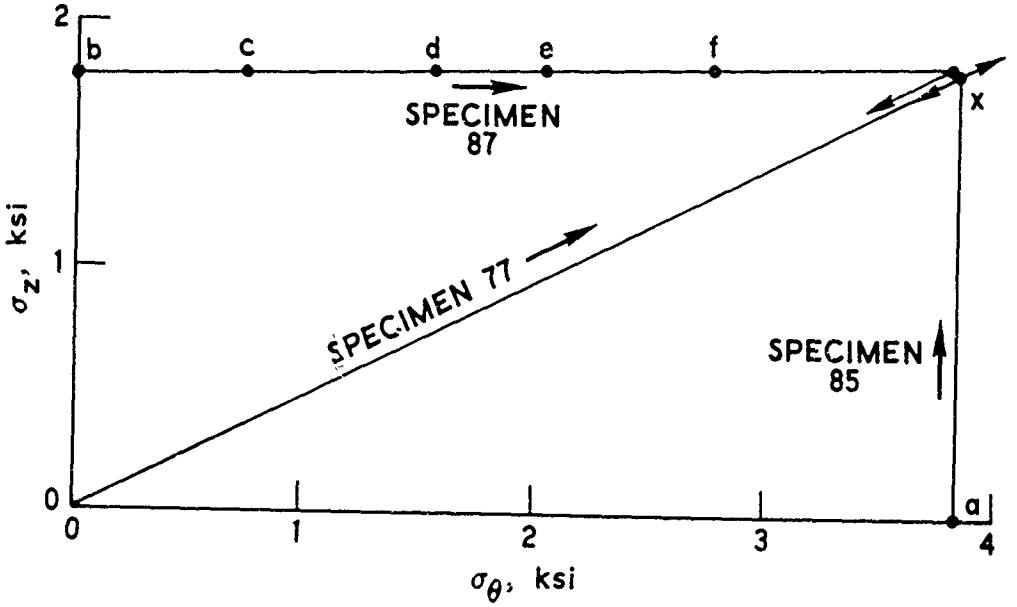

Fig. 5. Stress Trajectories for Biaxial Softening Tests (adapted from reference cited in footnote 5)

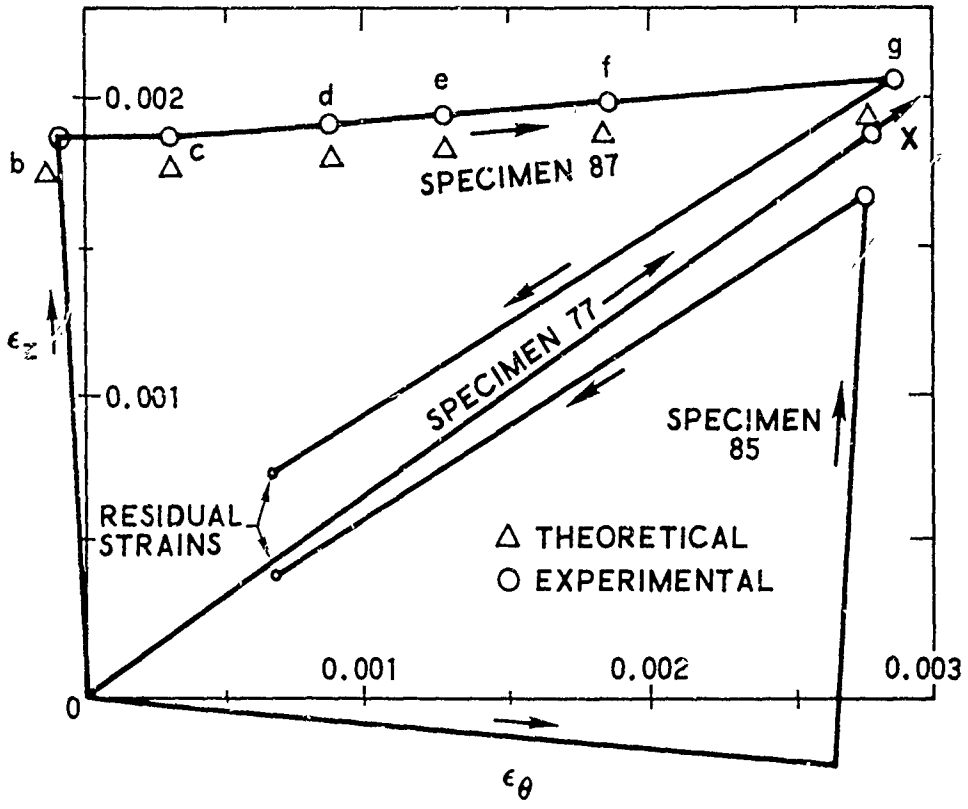

Fig. 6. Strain Trajectories (as given in reference cited in footnote 5) Compared with Theoretical Points

incremental theory would lead to larger discrepancies with the experiment than would application of the present theory without consideration of the loading path. The latter procedure therefore appears to be indicated until a more complete understanding of the path dependence question is available.

V. RELATION TO OTHER STRESS-STRAIN LAWS

Three polyaxial stress-strain laws have previously been proposed for transversely isotropic graphites. Here they will only be identified and briefly discussed, since a detailed comparison with the current approach and with test data is beyond the scope of this paper.

The first stress-strain law is due to Weng.[7] It states, in effect, that all strain components increase proportionally during proportional loading, an assumption that appears to be valid for compression, but only approximately true for tension. His function ϕ, which corresponds to our $(1 + F)$, was not formulated analytically and did not include contributions from shear stresses. His results therefore do not constitute a general stress-strain law, and in addition they seem not to be in as good agreement with the experiment as the present formulation.

An incremental-type theory patterned after classical plasticity theory was proposed by Weiler.[8] The theory explicitly treats thermal as well as load-induced stresses and assumes a bilinear or trilinear stress-strain relation. However, the present author believes that the experiments cited in footnote 5 invalidate the incremental plasticity theory for ATJS-type graphite. The use of incremental plasticity theory is therefore unwarranted, particularly when the additional complexity of incremental theories is taken into consideration.

Jones and Nelson[9] have proposed a deformation-type theory in which the various material parameters appearing in Eq. (1) are independently

variable with the stress and strain level. The rotational invariance requirement is met by relating the values of those parameters to the contracted matrix product of the stress and strain tensors. This approach appears to be a good deal more complicated to apply than that advanced in this paper. In the author's view, the success of the present approach makes the additional complications questionable, especially as it is not clear that any greater accuracy would result.

VI. DISCUSSION

This paper presents a new, nonlinear, polyaxial stress-strain relation for ATJS-type graphites that reduces to the known elastic relations at low stresses and is in good agreement with extensive biaxial and triaxial data at higher stresses. It is a deformation-type theory, which means it is strictly applicable only to proportional loading. However, it gives a rather good approximation (better than simple classical incremental theories) even in nonproportional loading. The author believes that, although this theory was formulated to apply specifically to ATJS, with minor changes in moduli and Poisson's ratios it can also be used for related graphites.

As written, the equations give strains as functions of the stresses. Because of the nonlinear coupling between the stresses, an exact analytical formulation of the stresses in terms of strains is not practicable. However, the problem can readily be solved iteratively as follows. Given the strains, an arbitrary numerical value for F (such as 0.5) can be assumed. This converts the equations into a set of simultaneous linear algebraic equations that can readily be solved for the stresses. With these stress values, a corrected value for F can be computed and the process repeated, continuing until a satisfactory degree of convergence is achieved.

In summary, the analytical formula for the polyaxial stress-strain relations of ATJS proposed here is a generalization, guided by theoretical considerations, of a large amount of test data. The result is neither rigorous nor unique, but it is simple, surprisingly accurate, and relatively easy to use. It should, therefore, be of value in structural analysis.

FOOTNOTES

[1]J. Jortner, Biaxial Mechanical Properties of ATJ-S Graphite, MDC G2072, McDonnell Douglas Astronautics Co., Huntington Beach, Calif. (December 1970).

[2]J. Jortner, Multiaxial Behavior of ATJ-S Graphite, AFML-TR-71-160, Air Force Materials Laboratory, Wright-Patterson AFB, Ohio (July 1971).

[3]J. Jortner, Multiaxial Behavior of ATJ-S Graphite, AFML-TR-71-253, Air Force Materials Laboratory, Wright-Patterson AFB, Ohio (December 1971).

[4]J. Jortner, Uniaxial and Biaxial Stress-Strain Data for ATJ-S Graphite at Room Temperature, MDC G3564, McDonnell Douglas Astronautics Co., Huntington Beach, Calif. (June 1972).

[5]J. Jortner, Multiaxial Response of ATJ-S Graphite, AFML-TR-73-170, Air Force Materials Laboratory, Wright-Patterson AFB, Ohio (October 1973).

[6]S. G. Lekhnitskii, Theory of Elasticity of an Anisotropic Elastic Body, Holden-Day Inc., San Francisco, 1963.

[7]T. L. Weng, "Biaxial Fracture Strength and Mechanical Properties of Graphite-Base Refractory Composites," Am. Inst. Aeron. Astronautics J. 7 (5), 851-858 (1969).

[8]F. C. Weiler, "Anisotropic Elastic-Plastic-Thermal Stress Analysis of Solid Structures," Proceedings First International Conference on Structural Mechanisms in Reactor Technology, Berlin, Sept. 20-24, 1972.

[9]R. M. Jones and D. A R. Nelson, Jr., "A New Material Model for the Inelastic Biaxial Behavior of ATJ-S Graphite," Proceedings AIAA/ASME/SAE 15th Structures, Structural Dynamics, and Materials Conference, Las Vegas, Nev., April 17-19, 1974.

LABORATORY OPERATIONS

The Laboratory Operations of The Aerospace Corporation is conducting experimental and theoretical investigations necessary for the evaluation and application of scientific advances to new military concepts and systems. Versatility and flexibility have been developed to a high degree by the laboratory personnel in dealing with the many problems encountered in the nation's rapidly developing space and missile systems. Expertise in the latest scientific developments is vital to the accomplishment of tasks related to these problems. The laboratories that contribute to this research are:

Aerophysics Laboratory: Launch and reentry aerodynamics, heat transfer, reentry physics, chemical kinetics, structural mechanics, flight dynamics, atmospheric pollution, and high-power gas lasers.

Chemistry and Physics Laboratory: Atmospheric reactions and atmospheric optics, chemical reactions in polluted atmospheres, chemical reactions of excited species in rocket plumes, chemical thermodynamics, plasma and laser-induced reactions, laser chemistry, propulsion chemistry, space vacuum and radiation effects on materials, lubrication and surface phenomena, photosensitive materials and sensors, high precision laser ranging, and the application of physics and chemistry to problems of law enforcement and biomedicine.

Electronics Research Laboratory: Electromagnetic theory, devices, and propagation phenomena, including plasma electromagnetics; quantum electronics, lasers, and electro-optics; communication sciences, applied electronics, semiconducting, superconducting, and crystal device physics, optical and acoustical imaging; atmospheric pollution; millimeter wave and far-infrared technology.

Materials Sciences Laboratory: Development of new materials; metal matrix composites and new forms of carbon; test and evaluation of graphite and ceramics in reentry; spacecraft materials and electronic components in nuclear weapons environment; application of fracture mechanics to stress corrosion and fatigue-induced fractures in structural metals.

Space Physics Laboratory: Atmospheric and ionospheric physics, radiation from the atmosphere, density and composition of the atmosphere, aurorae and airglow; magnetospheric physics, cosmic rays, generation and propagation of plasma waves in the magnetosphere; solar physics, studies of solar magnetic fields; space astronomy, x-ray astronomy; the effects of nuclear explosions, magnetic storms, and solar activity on the earth's atmosphere, ionosphere, and magnetosphere; the effects of optical, electromagnetic, and particulate radiations in space on space systems.

THE AEROSPACE CORPORATION
El Segundo, California